International Journal of Advances in Engineering and Management (IJAEM)
Volume 3, Issue 10 Oct 2021, pp: 513-520 www.ijaem.net ISSN: 2395-5252

Design and Development of MPPT System Capable Of Increasing Energy Harvesting Efficiencies of SPV Installations

M. B. Abubakar[3] I.G. Saidu[1], A.A. Adeboye[2], and A. S. Mindaudu[3]

1 Usmanu Danfodiyo University Sokoto
2 Air Force Institute of Technology, Kaduna
3 Umaru Ali Shinkafi Polytechnic, Sokoto

Submitted: 01-10-2021 Revised: 10-10-2021 Accepted: 12-10-2021

ABSTRACT
In spite of the numerous advantages associated with solar power systems, they still do not present desirable efficiencies. A solar cell has a nonlinear voltage-current (V-I) characteristic, and the operating condition of the maximum solar power delivered from the solar cell varies according to solar illumination and cell temperature. To effectively use solar power, a maximum power condition needs to be tracked by a maximum power point tracking (MPPT) control. In this paper, an instrument is designed and developed to track the maximum power point of a PV installation capable of increasing its energy harvesting efficiencies. Several sensors were employed to measure the characteristics of the solar panels. In addition, a custom circuit for automatic switching between different MPPT algorithms was developed. The system performed quite well and was able to enhance a tested PV efficiency. Further enhancement could be achieved if the system is combined with a machine learning capability to enable the system automatically "learn" the constants required for optimal operation. The integration of the MPPT system with mechanical solar trackers will enable optimal positioning relative to the irradiation source.

I. INTRODUCTION

Recently, energy generated from clean, efficient, and environmentally-friendly sources has become one of the major challenges for engineers and scientists. Among all renewable energy sources, solar power systems attract more attention because they provide excellent opportunity to generate electricity while greenhouse emissions are reduced. It is also gratifying to lose reliance on conventional electricity generated by burning coal and natural gas. Regarding the endless aspect of solar energy, it is worth saying that solar energy is a unique prospective solution for energy crisis. However, despite all the aforementioned advantages of solar power systems, they do not present desirable efficiency. (Bonnelle, 2004)

While technologies have pushed the conversion efficiency of solar cells up, the upper limit is still between 28 and 30%, making the generated energy only marginally-competitive at $0.10 per kilowatt-hour (kWh) compared to fossil-generated electricity within a $0.05 to $0.17 per kWh (Dominic, 2018).

The need of the hour is to extract maximum power from an SPV system regardless of prevailing environmental conditions to offset the inherent low conversion efficiency, demanding that the last watt be "squeezed" out of any PV generator.

When harvesting solar energy by the means of electrical solar cells, several parameters must be optimized to attain the maximum power possible at that level of solar radiation. One of the main issues is that the power obtained from a solar cell varies with the electrical load applied to the cell, and it is therefore important to operate at a load that gives maximal power. This operating point is affected by numerous conditions, these include temperature, light intensity and light incidence angle.

A maximum power point tracker is an optimizing circuit that is used in conjunction with PV power generators to achieve the maximum delivery of power from the generator to the load. Modern MPPTs typically include a microcontroller (MCU) that is responsible for detecting the MPP,

International Journal of Advances in Engineering and Management (IJAEM)
Volume 3, Issue 10 Oct 2021, pp: 513-520 www.ijaem.net ISSN: 2395-5252

and a power converter that ensures the generator's output satisfies the load requirements (Stephenson, 2012).

The focus of this dissertation is to develop a Maximum Power Tracking System that is capable of increasing energy harvesting efficiencies of solar photovoltaic installations. This will help in identifying the maximum power from a solar panel with minimal losses, with minimal upsets as a result of environmental vagaries that affects the conversion efficiency. The characteristics of the solar panels are measured using several sensors, and a custom circuit for automatic switching between MPPT algorithms.

II. MATERIALS AND METHODS

2.1 DC-DC Converter

Switched-mode DC-DC converters are used to convert the unregulated DC input into a controlled DC output at a desired voltage level. The relationship of transformation in a DC transformer can be controlled electronically by changing the duty cycle of the converter within the range 0 to 1(Rahman et al, 2012).

2.2 System Design

A block diagram of the system is shown in Figure 1 which comprised the following components:

a. Solar PV module
b. DC Load (12-volt Battery)
c. DC-DC Buck Converter
d. STM32F103C8 MCU

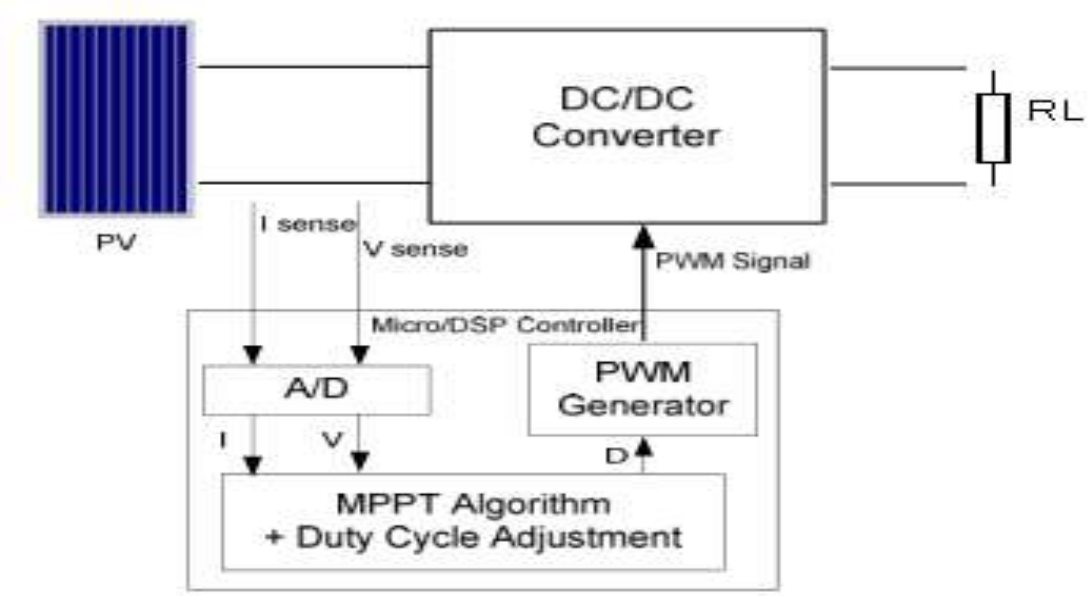

Figure 1: MPPT block diagram

Table 1: System design specifications

Specifications	Unit	Value
$\mathbf{V_{INmax}}$	V	36
$\mathbf{I_{INmax}}$	A	20
Frequency	Hz	100k
$\mathbf{V_{OUT}}$	V	28.8
$\mathbf{I_{LMAX}}$	A	10
$\mathbf{\Delta I_L}$ **(30% $\mathbf{I_L}$)**	A	3
$\mathbf{\Delta V_{out}}$ **(0.05% $\mathbf{V_{OUT}}$)**	mV	14.4

International Journal of Advances in Engineering and Management (IJAEM)
Volume 3, Issue 10 Oct 2021, pp: 513-520 www.ijaem.net ISSN: 2395-5252

2.3 PV Module Selection

The choice of module short-circuit current was dictated by the current-handling capability of the inductor used in the buck converter section. Two separate inductors were connected in series to increase the effective inductance value, and also split the current load. The inductors chosen were designed to handle 10 Amps continuously, therefore the short-circuit current (I_{sc}) of the module was mandated to be below 20A.

However, since all modules, regardless of manufacturing technology, are subject to external environmental variables, it then implies that any type of solar module can be selected for use as a solar collector for this study. In this research a polycrystalline silicon solar module manufactured by SL SOLAR AP-PM-50 with total area of 1.08m^2 was deployed. The specifications are given in Table 2.

Table 2: Photovoltaic module specifications

Parameters	Rating
Maximum power (P_{max})	50 W
Output tolerance	±5 %
Current at Pmax (I_{mp})	2.85 A
Voltage at Pmax (V_{mp})	17.5 V
Short-circuit current (I_{sc})	8.32 A
Open-circuit voltage (V_{oc})	22.05 V
Active surface area	0.35 m^2
Fill factor (FF)*	0.271864
Efficiency	14.286 %

2.4 Voltage Measurement

Measurement of panel voltage was effected using resistive components. The PV panel voltage was measured using resistive attenuators shown in Figure 2..

The rationale behind this was simplicity and flexibility. Since the system itself was low-voltage by design, there was no need for isolation of the input front-end from the signal processing back-end, hence the direct interfacing of the panel to the MCU using resistors.

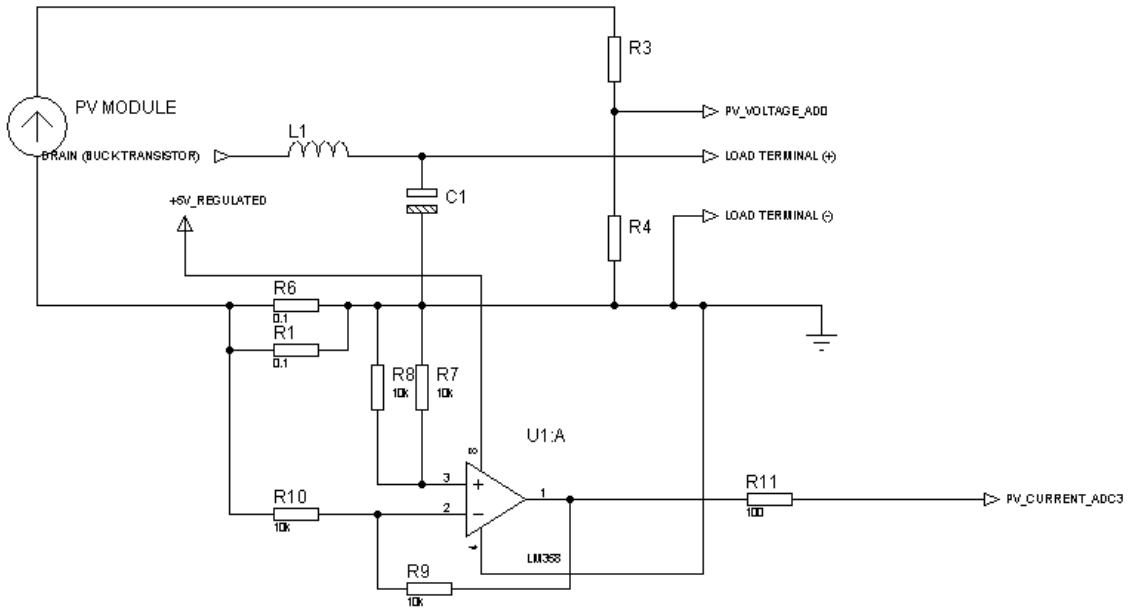

Figure 2: Resistive potential dividers for voltage and current measurements.

Power generated by the PV module was computed as the product of the PV voltage and PV current, and used in the MPP tracking control loop.

2.5 Current Measurement

International Journal of Advances in Engineering and Management (IJAEM)
Volume 3, Issue 10 Oct 2021, pp: 513-520 www.ijaem.net ISSN: 2395-5252

Current was measured using the simplest current-to-voltage converter: a resistor. Two 0.1 Ohm 10-watt power resistors were connected in parallel for an increased current sensing range of 20A, and place in the ground return of the PV ground. Current flowing through the system (and through the buck converter) developed a voltage across the resistor, the value of which is directly proportional to the product of the magnitude of the resistance and the current.

$V_{sense} = I_{pv} \cdot R_{sense}$

Where

V_{sense} = voltage developed across the resistance

I_{pv} = current flowing through the MPPT from the PV module

R_{sense} = value of the current-sensing resistor.

The maximum current measurable by the power resistor is dictated by its upper limit on power dissipation. Using the specified 10 Watts of dissipation, the maximum current measurable is given by

$P = I^2R$

Using a value of 0.1 ohms, the maximum current measurable is 10 Amps.

Since two resistors of similar specifications were paralleled, the maximum measurable current was effectively doubled to 20A. This was also the maximum current the inductors could handle.

2.6 STM32F103C8 32-Bit Arm Microcontroller

The STM32F103xB series is a performance line ARM-based 32-bit MCU.The ARM family of MCUs is designed to meet low-power high-computational needs of computer systems, and can be found in mobile phones, electronic gadgets, satellite receivers, and other embedded computer systems (Figure 3).

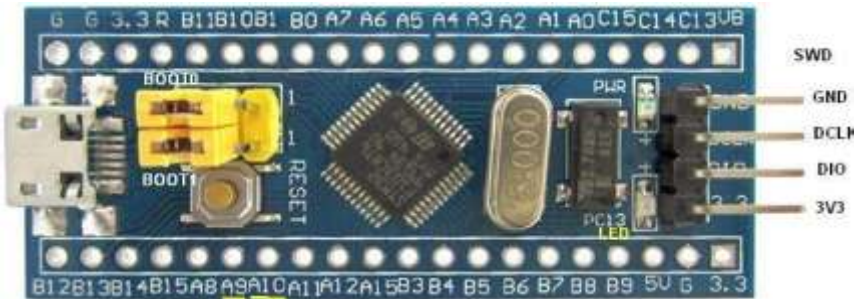

Figure 3: STM32F103C8 ARM on breakout board (ST Microelectronics, 2007)

2.7 STM32F103C8 ADC Subsystem

The STM32F103 MCU sports a 12-bit successive approximation register (SAR) analog-to-digital converter. It has up to 19 multiplexed channels allowing it to measure signals from 16 external sources, two internal sources, and the VBAT channel. The A/D conversion of the channels can be performed in single, continuous, scan or discontinuous mode. The result of the ADC is stored into a left-or right-aligned 16-bit data register.

An analog watchdog feature allows the application to detect if the input voltage goes beyond the user-defined, higher or lower thresholds.

2.8 LM358 Operational Amplifier

The LM358 was used as an inverting amplifier in the research work in conjunction with the current sense resistor. Figure 4 is the pin identification for LM358 IC used.

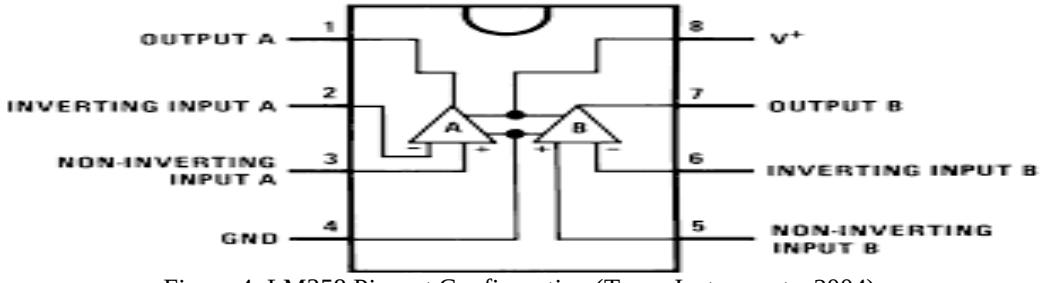

Figure 4: LM358 Pin-out Configuration (Texas Instruments, 2004)

International Journal of Advances in Engineering and Management (IJAEM)
Volume 3, Issue 10 Oct 2021, pp: 513-520 www.ijaem.net ISSN: 2395-5252

IRFP4905 P-Channel Power MOSFET

A P-channel MOSFET was used in the design of the buck converter as it presented fewer gate drive challenges relative to the N-channel counterpart. The IRFP4905 part is capable of handling a continuous drain current of 74 Amps, at a drain-source voltage of -55V.

2.9 Buck Converter Design

This section provides all the calculations required to implement a buck converter..

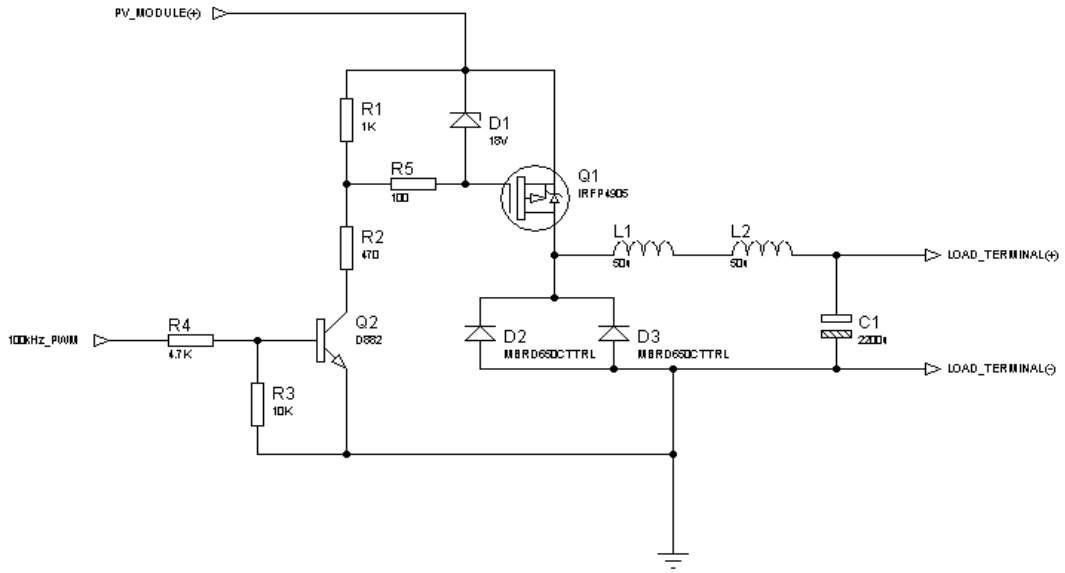

Figure 5: Buck converter transistor drive

2.10 Experimental Test Bed

The test bed for evaluating the performances of these algorithms is shown in Plate 1. It embodied the test PV module, a KIPP&ZONEN CMP3 pyranometer, the MPPT hardware, and a 12-volt 40AH battery serving as the load.

The test bed was placed away from every aerial obscurant capable of skewing the measured data sets, thus presenting a non-biased platform for further comparison and analysis.

Data was recorded to the attached Secure Digital (SD) card every 10 seconds, this being the frequency of computation of the MPPT gain.

The data sets were recorded under clear bright skies. Each data entry was date- and time-stamped for date- and time-based analyses.

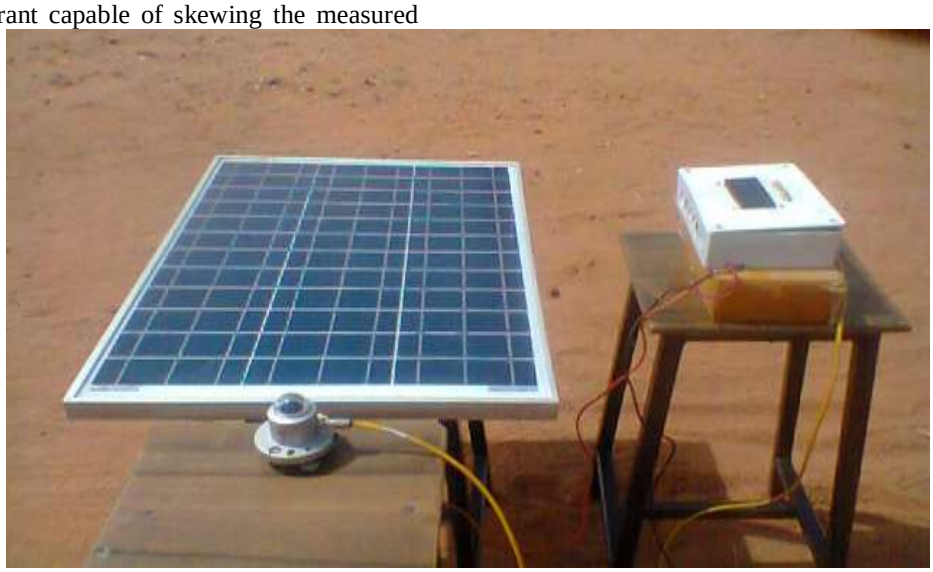

Plate 1: MPPT evaluation test bed

International Journal of Advances in Engineering and Management (IJAEM)
Volume 3, Issue 10 Oct 2021, pp: 513-520 www.ijaem.net ISSN: 2395-5252

The embedded system on which the algorithms were tested is shown in Plate 2.

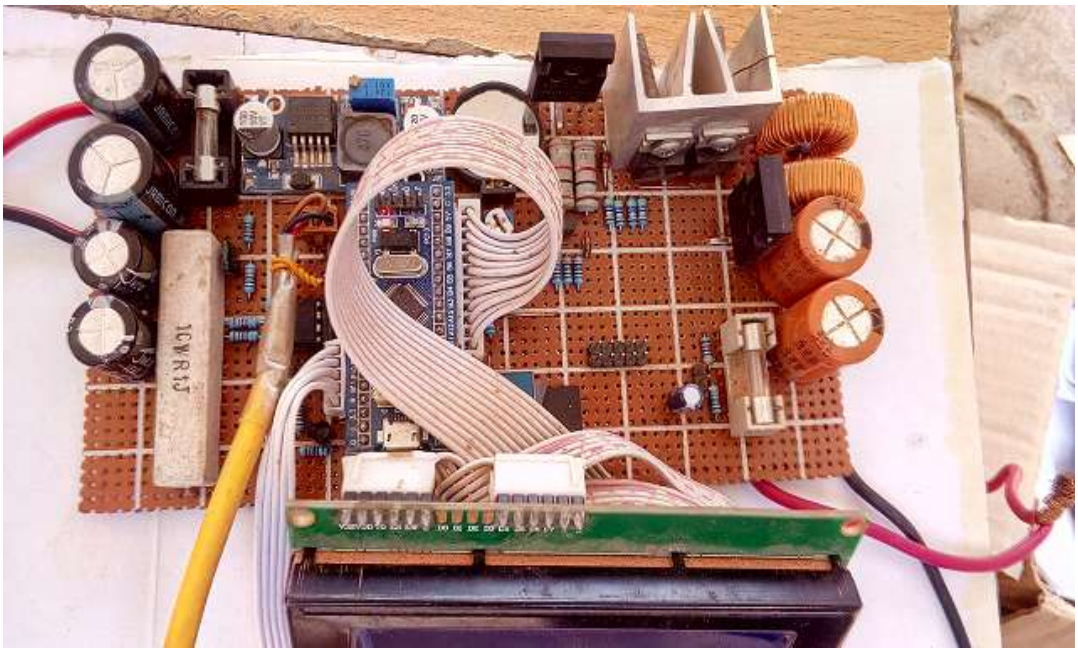

Plate 2: MPPT algorithm evaluation hardware

III. RESULTS AND DISCUSSION

3.1 Result

Tables 3 and 4 present the raw logs and the logs after adjustment to standard irradiance of 1000W/m^2.

Table .3: Raw log data sets for tested algorithms

DATE	MPPT	G_{MAX} (W/M^2)	G_{MIN} (W/M^2)	G_{AVG} (W/M^2)	$POWER_{MPPT}$ (W)	$POWER_{NON-MPPT}$ (W)	MPPT GAIN (%)	LOG COUNT
20-12-17	P&O	703.29	35.46	352.62	15.30	13.50	13.34	9806
21-12-17	PS	706.25	73.88	327.74	15.33	12.17	25.93	1921
22-12-17	FOCV	729.89	35.46	394.34	17.47	14.53	20.20	11197
23-12-17	IC	747.62	17.73	307.02	13.19	11.80	11.77	10470
31-12-17	P&O	723.98	23.64	429.41	18.42	16.34	12.70	11623
01-01-18	PS	511.22	29.55	308.84	14.39	11.01	30.68	2156
05-01-18	FOCV	712.16	23.64	417.71	18.26	15.17	20.37	11733
24-01-18	IC	865.82	73.88	516.78	2.78	2.50	11.18	11870
05-02-18	P&O	809.67	26.60	551.52	22.71	19.68	15.41	8441
06-02-18	PS	839.22	47.28	565.54	24.10	19.36	24.52	2159
07-02-18	FOCV	966.29	106.38	679.51	25.70	18.74	37.11	12012

International Journal of Advances in Engineering and Management (IJAEM)
Volume 3, Issue 10 Oct 2021, pp: 513-520 www.ijaem.net ISSN: 2395-5252

10-02-18	IC	759.44	32.51	516.68	19.40	17.45	11.19	11771
03-06-18	MPS	859.10	100.46	458.20	18.77	15.97	17.51	2876
04-06-18	MPS	812.63	38.42	518.38	19.03	15.93	19.44	2928
08-06-18	MPS	517.59	58.82	250.96	16.35	14.28	14.47	3042
13-06-18	MPS	523.47	14.780	211.22	13.67	11.62	17.70	2599
14-06-18	MPS	561.70	58.80	233.70	14.71	11.91	23.48	2875

Table 4: Processed data adjusted for standard (1000W/m^2) irradiance

DATE	MPPT	$POWER_{MPPT}$ (W)	$POWER_{NON-MPPT}$ (W)	MPPT GAIN (%)	MPPT EFFICIENCY (%)
20-12-17	P&O	42.94	37.49	14.49	85.86
21-12-17	PS	47.50	36.31	30.82	95.00
22-12-17	FOCV	42.98	34.64	24.08	85.96
23-12-17	IC	43.16	38.31	12.65	86.31
31-12-17	P&O	41.03	36.32	12.96	82.05
01-01-18	PS	46.04	34.50	33.45	92.07
05-01-18	FOCV	43.91	34.70	26.55	87.82
24-01-18	IC	7.73	6.95	11.22	15.45
05-02-18	P&O	40.49	34.94	15.88	80.98
06-02-18	PS	43.47	33.27	30.66	86.95
07-02-18	FOCV	38.15	26.67	43.06	76.30
10-02-18	IC	35.19	31.65	11.20	70.39
03-06-18	MPS	43.67	37.15	17.55	87.33
04-06-18	MPS	39.64	33.59	18.02	79.28
08-06-18	MPS	59.12	51.91	13.88	118.24
13-06-18	MPS	66.22	56.26	17.72	132.45
14-06-18	MPS	56.94	46.47	22.54	113.89

3.2 DISCUSSION

The raw data sets for the tested algorithms are given in Table 3. Average values of the measured and computed parameters are given along with the performance figures of each algorithm. As the data sets were not yet adjusted for standard test conditions, comparison can only be made between the MPPT-driven and baseline non-MPPT power extraction performances. Worthy of observation is the fact that the power generated is directly related to the level of irradiance to which the test bed was exposed to during logging.

It is important to observe that the uncertainties in the PV voltage and current measurements and the small differences in the environmental conditions between each test suggest that the results cannot be a good reference to calculate the efficiency of the single MPPT algorithm. In these conditions, even an uncertainty of 0.5% in the measurements could produce an uncertainty in the relative power losses that could be more than 10%. (Dolara et al, 2009). While it may seem that translating the measured parameters to STC should generate data sets of high integrity, the non-availability of two important characteristics of PV modules – voltage coefficient of temperature and current coefficient of temperature – will greatly affect the accuracy of computed performances. They were assumed negligible in this research, but this assumption may be violated at high irradiance levels with corresponding elevated panel temperature rise.

Most of the literatures cited quoted efficiency values derived from simulated atmospherics, without the hard parameters involved in outdoor operational testing. However in some literatures, experimental validations were established, making a fair comparison possible with the result derived in the algorithms developed in this research.

The first run of the test yielded an average MPPT-derived power harvest of 15.30W compared to 13.50W baseline for the P&O algorithm, corresponding to an MPPT net gain of 13.34%. Figure for the PS implementation was similar at 15.33W MPPT-derived power production relative to 12.179W for the reference baseline energy extraction implementation. This translated into a 25.93% MPPT overall gain. The FOCV MPPT alternative netted a 20.20% MPPT boost. The IC algorithm performed slightly lower than the other three algos, with an MPPT gain of 11.77%.

The results of the second test mirrored the first test, with the MPPT boost coming in at 12.70%, 30.68%, 20.37%, and 11.18% for the P&O, PS, FOCV, and IC respectively. As expected, the power produced by the sweep algorithm was markedly higher than others since it was always guaranteed to locate the MPP. The FOCV algorithm came in as a strong contender in term of the gain performance, with a figure better than both P&O and IC.

Test run three showed the FOCV method extracting more power than other algorithms, at a gain boost of 37.10%.The P&O, PS, and IC exhibited gains of 15.41%, 24.52%, and 11.19%. The MPS algorithm reported power gains of 17.50%, 19.44, 14.47%, 17.70%, and 23.48%, for five runs conducted. The lowest irradiance levels were encountered during these runs, and should be taken into cognizance.

IV. CONCLUSION

This study presents a design of an instrument capable of comparing the maximum power point tracking efficiencies of different MPPT control algorithms, and the performance evaluation of MPS algorithm. The Results of the experiments carried out to test the instrument showed that the PS MPPT, though not the most widely-adopted method, provided the most performance, with the potential to be competitive if minimal losses can be tolerated in operation, and if semiconductor switches with ultra-high level of thermal-handling capability can be utilized.

REFERENCES

[1]. Bonnelle, D.(2004). “Solar Chimney, Water Spraying Energy Tower, and Linked Renewable Energy Conversion Devices:presentation, criticism and proposals”, Doctorate Dissertation, University Claude Bernard - Lyon 1 – France

[2]. Dolara,A., Faranda, R., and Leva, S. (2009), “Energy Comparison of Seven MPPT Techniques for PV Systems”, Journal of Electromagnetic Analysis & Applications, 3: 152-162.

[3]. Dominic Dudley. (2018). “Renewable Energy Will Be Consistently Cheaper Than Fossil Fuels by 2020”. Retrieved from https://www.forbes.com/sites/dominicdudley/2018/01/13/renewable-energy-cost-effective-fossil-fuels-2020/#43d7255e4ff2 on July 10, 2018.

[4]. Rahman, S., Oni, N. S., and Ibn Masud, Q. A.(2012).“Design of a Charge Controller Circuit with Maximum Power Point Tracker for Photovoltaic System,” Dept. of Electrical & Electronic Engineering, BRAC University.

[5]. Stephenson, Christopher A., (2012).“Utilizing maximum power point trackers in parallel to maximize the power output of a solar (photovoltaic) array”,MSc. Dissertation, Naval Postgraduate School, Monterey, California.

[6]. ST Microelectronics. (2007).STM32F103x6, STM32F103x8, STM32F103xB Performance line, ARM-based 32-bit MCU Preliminary Data.www.st.com.

[7]. Texas Instruments, (2004).LM358 Dual Operational Amplifier.www.ti.com.